

# Monitoring of amorfization of the oxygen implanted layers in silicon wafers using photothermal radiometry and modulated free carrier absorption methods

M. Maliński · M. Pawlak · Ł. Chrobak ·  
S. Pal · A. Ludwig

Received: 20 July 2014 / Accepted: 27 October 2014 / Published online: 12 November 2014  
© The Author(s) 2014. This article is published with open access at Springerlink.com

**Abstract** This paper presents experimental results that characterize implanted layers in silicon being the result of a high energy implantation of  $O^{+6}$  ions. We propose a simple relation between attenuation of photothermal radiometry and/or modulated free carrier absorption amplitudes, the implanted layer thickness and its optical absorption coefficient. The thickness of the implanted layers was determined from capacitance–voltage characteristics and computations with the TRIM program. The obtained results allowed to estimate changes of the optical absorption coefficient of the oxygen implanted layers indicating the amorfization of the layers.

## 1 Introduction

The ion implantation process is a very important technological process in the semiconductor industry. Measurement methods based on plasma waves are very attractive for monitoring electrical transport parameters (carrier diffusivity, lifetime of carriers and surface recombination velocities of carriers) in the ion implanted layer as well as in the substrate. Plasma waves can be detected by the

measurement of the periodical component of the intensity of the IR radiation of the samples, in a PTR method, or by the measurement of the intensity of the periodical component of the transmitted probing IR beam of light in a MFCA method, or by the periodical photoluminescence in a photocarrier radiometry (PCR) method [1–3]. Analysis of the frequency characteristics enables determination of the recombination parameters of semiconductors with the PTR method [4, 5] and the MFCA method [6–12]. For one layer samples, it is possible to determine the lifetime of carriers and the velocity of the surface recombination from the frequency amplitude and phase PTR or MFCA characteristics. In paper [13], the influence of  $O^{+6}$  ion implantation on the recombination parameters of n-type Si samples, investigated with the PTR method, was presented. With the increase of ion implantation doses (1) the substrate recombination lifetimes and the carrier diffusivity were unchanged; (2) the surface recombination velocity increased and (3) the parameter  $A$ , which described the relative plasma and thermal contributions, increased. In this paper, we present the correlation between damping of the plasma component of the PTR signal and the thickness of the  $O^{+6}$  ion implanted layer in n-type silicon samples. For implanted samples, these methods enable determination of changes of the optical absorption coefficient of implanted layers when their thickness is known.

## 2 Material and experimental setups

### 2.1 Materials

Table 1 presents resistivities, thicknesses of the n-type silicon samples and also parameters of the implantation process with the  $O^{+6}$  ions used in the investigations.

---

M. Maliński · Ł. Chrobak  
Department of Electronics and Computer Science,  
Koszalin University of Technology, 2 Śniadeckich St.,  
75-453 Koszalin, Poland

M. Pawlak (✉)  
Institute of Physics, Faculty of Physics, Astronomy  
and Informatics, Nicolaus Copernicus University,  
Grudziądzka 5/7, Toruń, Poland  
e-mail: mpawlak@fizyka.umk.pl

M. Pawlak · S. Pal · A. Ludwig  
Experimental Physics VI, Ruhr-University Bochum,  
Universitätsstrasse 150, 44780 Bochum, Germany

**Table 1** Properties of the n-type silicon samples implanted with the O<sup>+6</sup> ions and the parameters of implantation

Sample	Ions	Energy (keV)	Dose (ions/cm <sup>2</sup> )	Resistivity (Ω cm)	Thickness (cm)
n-Si	–	–	–	3–5	0.41
n-Si	O <sup>+6</sup>	90	5 × 10 <sup>13</sup>	–	0.41
n-Si	O <sup>+6</sup>	90	5 × 10 <sup>14</sup>	–	0.41

2.2 Experimental setups

The PTR experimental setup for the frequency PTR measurements of semiconductor samples in the reflection configuration was described elsewhere [5]. The experimental setup for the measurements of the frequency characteristics of the MFCA signal in a transmission configuration is presented in Fig. 1.

There are two sources of light in this setup. The first one is a pumping laser working at the wavelength 660 or 808 nm, exciting carriers from the valence band to the conduction band. Energy of photons of the pumping laser must be bigger than the value of the energy gap of the investigated semiconductor. The second source of light was a semiconductor laser working at the wavelength, λ = 1,600 nm as a probing laser. Energy of photons of the probing light must be smaller than the value of the energy gap of the semiconductor. The intensity of the probing beam of the laser light is constant in time. Intensity of the

pumping laser beam is modulated by the Thorlabs controller and a TTL signal of the lock-in amplifier. Measurements of the thickness of the implanted layers were taken on the experimental setup for capacitance–voltage measurements presented in Fig. 2.

In the measurements, the capacitance of the sample was measured as a function of the applied DC voltage in the range from –1 to 1 V, with a 10 mV step; 8 kHz sine signal was superimposed to the DC voltage. The thickness of the oxide layer was calculated from the accumulation region capacitance, where the sample behaves as a simple capacitor.

3 Theoretical model

The PTR and MFCA signals can be written as follows [13]

$$PTR(f) \approx \frac{1}{f} \cdot \exp\left(-\frac{\pi}{2}i\right) + \frac{1}{A} \cdot \int_0^l \Delta n(x, f) dx, \tag{1}$$

$$MFCA(f) \approx \int_0^l \Delta n(x, f) dx, \tag{2}$$

where Δn(x) is a concentration of carriers, A is a thermal to plasma components coefficient, and l is the sample thickness. Magnitude of the plasma component depends on several material parameters (such as the absorption

**Fig. 1** Experimental setup for the measurements of the frequency characteristics of the MFCA signal in the transmission configuration

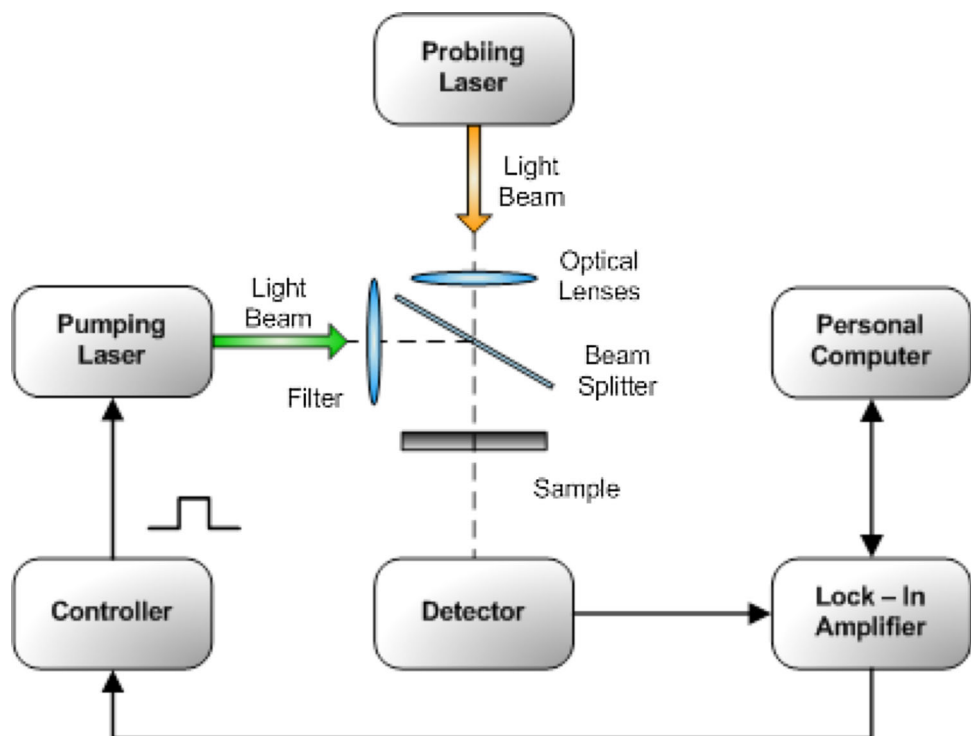
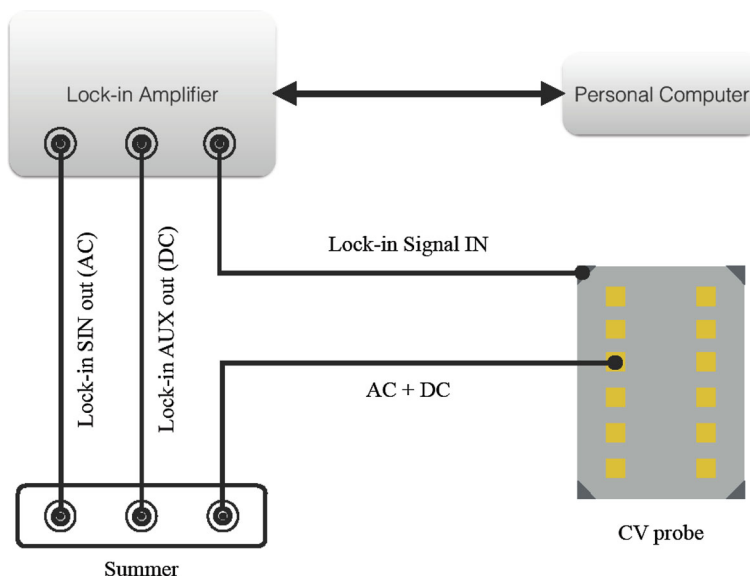


**Fig. 2** Experimental setup for the capacitance–voltage measurements. The sample was processed with a standard CV-mask, with Au-gates of 300 μm by 300 μm, shown as yellow squares in the figure. Indium contacts at the four corners of the CV probe were used as back contacts



coefficient, energy bandgap, carrier recombination lifetime, carrier diffusivity and surface recombination velocities) as well as on experimental condition such as the laser light intensity, energy of photons and the frequency of modulation. The light intensity in the homogenous sample can be written as follows

$$I(x) = I(0) \cdot \beta \cdot \exp(-\beta \cdot x), \tag{3}$$

where  $\beta$  is the optical absorption coefficient of the homogenous sample, and  $I(0)$  is the light intensity at the surface. In the ion implanted sample, however, the light intensity in the end of the ion implanted layer can be written as

$$I(d) = I(0) \cdot \exp(-\beta_{\text{imp}} \cdot d), \tag{4}$$

where  $\beta_{\text{imp}}$  is the optical absorption coefficient of the ion implanted layer, and  $d$  is the ion implanted layer thickness. Assuming that the recombination lifetime and diffusion of carriers in the implanted layer are much smaller than in the substrate, one can conclude that the contribution of the PTR signal from this layer to the total PTR signal in the plasma component dominating frequency region can be neglected. This means that the PTR or MFCA signal in the case of the implanted layer is proportional to the light intensity given by formula (2) and

$$|\text{PTR}_{\text{imp}}| \approx A \cdot I(0) \cdot \exp(-\beta_{\text{imp}} \cdot d). \tag{5}$$

In the case of the nonimplanted sample, the PTR or MFCA signal is proportional to the light intensity given by formula (1) and

$$|\text{PTR}_{\text{non-imp}}| \approx A \cdot I(0) \tag{6}$$

Introducing a parameter  $k$

$$k = \frac{|\text{PTR}_{\text{imp}}|}{|\text{PTR}_{\text{non-imp}}|}, \tag{7}$$

one can write

$$k = \exp(-\beta_{\text{imp}} \cdot d) \text{ or } \beta_{\text{imp}} = -\frac{\ln(k)}{d}. \tag{8}$$

Formula (8) is valid for optically opaque samples ( $\beta \cdot L \gg 1$ ). Using a two layer model given in [14], it is possible to test the validity of the proposed formula. Numerical simulations show that this is true when  $\tau_{\text{imp}} \ll \tau$ , diffusion length in the ion implanted layer  $L_e = \sqrt{D_{\text{imp}} \cdot \tau_{\text{imp}}} < d$  and the light penetration depth  $1/\beta_{\text{imp}} < d$ . Parameters used for calculation were  $\tau_{\text{impl}} = 10^{-9}$  s,  $\tau = 10^{-5}$ ,  $D_{\text{impl}} = 1$  cm<sup>2</sup>/s,  $D = 20$  cm<sup>2</sup>/s,  $L_e = 0.3$  μm,  $1/\beta = 1$  μm,  $d = 1$  μm.

#### 4 Experimental results and discussion

Figure 3 presents the frequency versus PTR amplitude and phase characteristics of the n-Si samples nonimplanted and implanted by O<sup>+6</sup> ions of the energy 90 keV with a dose  $5 \times 10^{14}$  ions/cm<sup>2</sup> and illuminated by the laser beam operating at wavelength  $\lambda = 488$  nm.

From the PTR experimental characteristics of oxygen implanted samples and the nonimplanted silicon sample, several recombination parameters were determined using theoretical model described by formula (2) and they are presented in Table 2.

Figure 4 presents the frequency versus MFCA amplitude and phase characteristics of the n-Si samples nonimplanted and implanted by O<sup>+6</sup> ions of the energy 90 keV

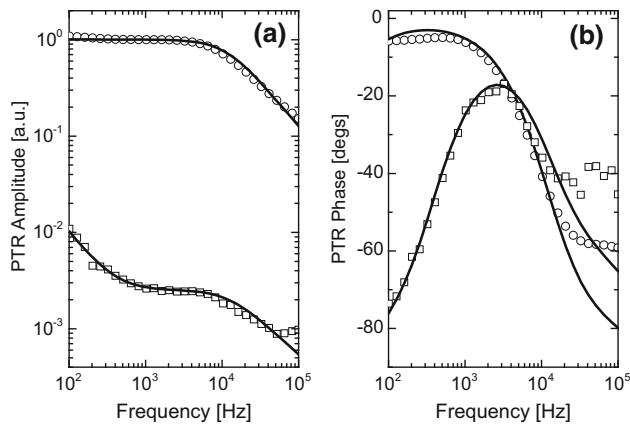


**Fig. 3** PTR amplitude normalized at  $f = 100$  Hz (a) and phase (b) frequency characteristics of nonimplanted n-type silicon sample (circles) and oxygen implanted with a dose  $5 \times 10^{14}$  ions/cm<sup>2</sup> sample for the wavelength  $\lambda = 488$  nm. Lines illustrate the fittings of theoretical curves described by formula (2) to experimental data

with a dose  $5 \times 10^{14}$  ions/cm<sup>2</sup> and illuminated by the laser beam operating at wavelength  $\lambda = 660$  nm and  $\lambda = 808$  nm.

Analysis of the experimental data led us to the conclusion that light absorbed in the oxygen implanted layer does not give its contribution to the PTR nor MFCA signals. Both PTR and MFCA signals come only from the silicon substrate. It can be explained with a very short life time of carriers in the implanted layer relative to the life time of carriers in the silicon substrate equal to  $\tau = 18$   $\mu$ s.

The model analysis led to the theoretical and experimental dependence presented in Fig. 5 where the parameter  $k$  is the ratio of the amplitudes of the PTR signal (for the wavelengths  $\lambda = 488$  and 514 nm) and MFCA (for the wavelengths  $\lambda = 660$  and 830 nm) of the implanted sample to the nonimplanted sample in the region of the domination of the plasma component of the PTR and MFCA signal over the thermal component, i.e., for the frequencies of modulation of the beam of light above  $f = 1$  kHz.

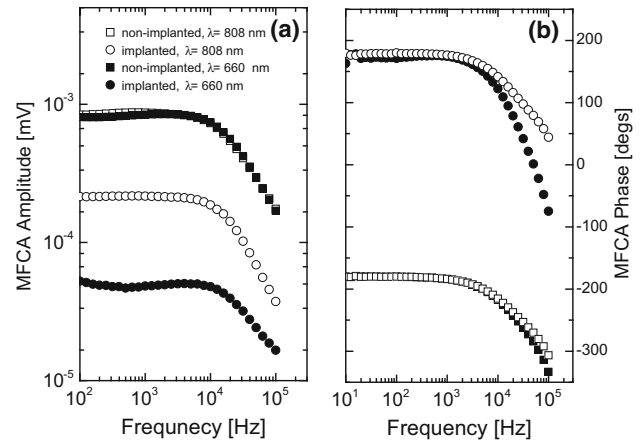


**Fig. 4** MFCA amplitude (a) and phase (b) frequency characteristics of nonimplanted n-type silicon sample (squares) and oxygen implanted samples (circles) with a dose  $5 \times 10^{14}$  ions/cm<sup>2</sup> for the wavelength  $\lambda = 660$  nm and  $\lambda = 808$  nm

From the character of the dependence, presented in Fig. 5, of the decrease of the PTR and MFCA signals with the energy of photons, it results that it is square in character what is characteristic for indirect electron type transitions in semiconductors. For determination of the value of the optical absorption coefficient of the implanted layers, the thickness of the implanted layer is necessary. The thickness of the layers was determined both from the capacitance measurements and TRIM computations. Values of the capacitances and the thicknesses of the implanted layers are presented in Table 3.

At the thickness of the implanted layer corresponding to the biggest dose of implantation  $5 \times 10^{14}$  cm<sup>-2</sup> determined from capacity measurements as  $d = 0.50509 - 0.12997 \mu\text{m} = 0.376 \mu\text{m}$  and the value  $\beta \cdot d = -\ln(k) = -\ln(1/145) = 5$ , for  $\lambda = 488$  nm determined from PTR measurements presented in Fig. 4, we get the average value of the optical absorption coefficient of the implanted layer equal to  $\beta = 13.2 \times 10^4$  cm<sup>-1</sup>. The value of the optical absorption coefficient of the nonimplanted silicon is equal

**Table 2** Recombination parameters of the n-type silicon nonimplanted and implanted samples with oxygen ions determined for  $\lambda = 488$  nm and  $\lambda = 514$  nm

Sample	Doze (ions/cm <sup>2</sup> )	Recombination lifetime $\tau$ ( $\mu$ s)	Diffusivity $D$ (cm <sup>2</sup> /s)	Surface recombination velocity $S_1$ (cm/s)	Surface recombination velocity $S_2$ (cm/s)	Parameter $A$ [1]
$\lambda = 488$ nm						
n-Si	–	18	12	400	1,000	$3 \times 10^{-6}$
n-Si:O	$5 \times 10^{14}$	18	12	2,500	1,000	$390 \times 10^{-6}$
$\lambda = 514$ nm [13]						
n-Si	–	18	12	400	1,000	$3 \times 10^{-6}$
n-Si:O	$5 \times 10^{13}$	18	12	1,800	1,000	$180 \times 10^{-6}$
n-Si:O	$5 \times 10^{14}$	18	12	2,500	1,000	$360 \times 10^{-6}$

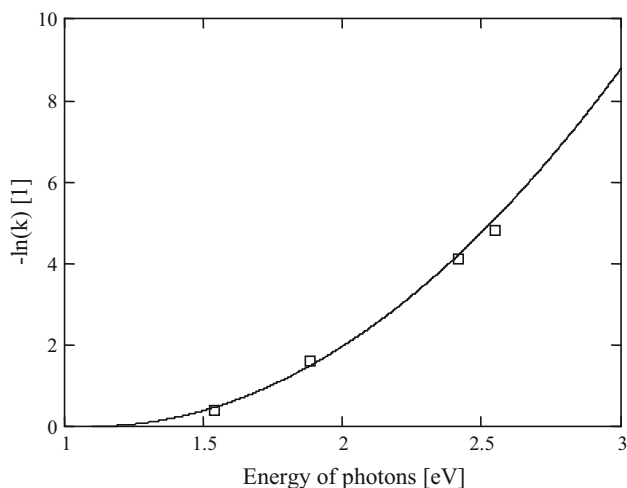


**Fig. 5** Dependence of  $-\ln(k)$  on the energy of absorbed photons for samples implanted with oxygen with a dose  $5 \times 10^{14}$  ions/cm<sup>2</sup>  $-\ln(k) = \beta_{\text{impl}} \cdot d = A \cdot (E_f - E_g)^2 \cdot d$  where,  $E_g = 1.1$  eV,  $A \cdot d = 2$

**Table 3** Thickness of the implanted layer determined by the C–V method

Samples	$C_{ox}$ (pF)	$d_{ox}$ (μm)
C17_nonimplanted	23.9	0.12997
C21 $5 \times 10^{14}$ cm <sup>-2</sup>	6.15	$0.50509 - 0.12997 = 0.376$

to  $\beta = 2 \times 10^4$  cm<sup>-1</sup> for  $\lambda = 488$  nm. It means 6.6 times increase of the value of the optical absorption coefficient of the implanted layer respective to the value of the optical absorption coefficient of silicon. The average value of the optical absorption coefficient in the implanted layer at the dose  $5 \times 10^{13}$  ions/cm<sup>2</sup> determined from the dependence  $\beta \cdot d = \ln(k) = -\ln(1/60) = 4$  from PTR measurements, and the same thickness of the implanted layer  $d = 0.376$  μm, is equal to  $10.6 \times 10^4$  cm<sup>-1</sup> and is 0.8 of the optical absorption value of the implanted layer at the dose  $5 \times 10^{14}$  cm<sup>-2</sup>. It means 5 times increase of the optical absorption coefficient of the implanted layer respective to silicon.

The ratio of the concentration spatial distribution of oxygen ions respective to the dose of implantation is presented in Fig. 6.

The depth of implantation of oxygen O<sup>+6</sup> ions computed in a TRIM program is equal to  $d = 0.376$  μm. It agrees with the values obtained from the C–V method. It gives an average value of the ratio  $\rho/\text{Dose} = 1/d = 2.66 \times 10^4$  cm<sup>-1</sup> where,  $\rho$  is the concentration of ions. At the dose  $5 \times 10^{14}$  ions/cm<sup>2</sup>, an average concentration of oxygen ions in the implanted layer  $\rho$  equals to  $13.3 \times 10^{18}$  ions/cm<sup>3</sup>, and it corresponds to the average value of the optical

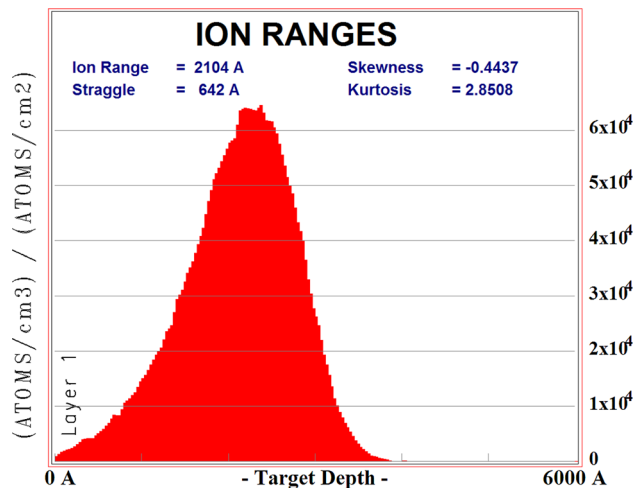


**Fig. 6** Spatial distribution of the ratio of concentration of oxygen ions in a silicon sample respective to the implantation dose computed in a TRIM program

absorption coefficient equal to  $\beta = 13.2 \times 10^4$  cm<sup>-1</sup> determined from the PTR measurements. Maximum concentration of oxygen ions at the depth 0.2 μm equals to  $32.5 \times 10^{18}$  ions/cm<sup>3</sup>. At the dose  $5 \times 10^{13}$  ions/cm<sup>2</sup>, the average concentration of oxygen ions equals to  $13.3 \times 10^{17}$  ions/cm<sup>3</sup>, and it corresponds to the average value of the optical absorption coefficient equal to  $\beta = 10.6 \times 10^4$  cm<sup>-1</sup> determined from the PTR or MFCA measurements. Maximum concentration of oxygen ions in the implanted layer equals to  $32.5 \times 10^{17}$  ions/cm<sup>3</sup> at this dose.

### 5 Conclusions

In this paper, the procedure of determination of the optical absorption coefficient of the O<sup>+6</sup> ions implanted layer is presented. The procedure is based on the frequency measurements of the PTR or MFCA signals of the implanted and nonimplanted silicon samples and determination of the thickness of the implanted layer from the C–V experiment or a TRIM program. Such information is essential from the point of view of evaluation of the degree of amorfization of the implanted layer. For the investigated implanted layers, a considerable increase of the optical absorption coefficient was determined. For the implantation dose  $5 \times 10^{14}$  ions/cm<sup>2</sup>, the optical absorption coefficient in the implanted layer increased 6.6 times respective to that of a silicon substrate. For the implantation dose  $5 \times 10^{13}$  ions/cm<sup>2</sup>, the optical absorption coefficient increased 5 times respective to that of the silicon substrate. The values of

the optical absorption coefficient are the measure of the amorfization of the implanted layer.

**Acknowledgments** Authors thank Prof. J. Pelzl from the Ruhr University in Bochum Germany for the possibility of measurements of PTR characteristics on the experimental setup in his laboratory and Prof. D. Todorovic for the samples.

**Open Access** This article is distributed under the terms of the Creative Commons Attribution License which permits any use, distribution, and reproduction in any medium, provided the original author(s) and the source are credited.

## References

1. A. Mandelis, J. Batista, J. Gibkes, M. Pawlak, J. Pelzl, *J. Appl. Phys.* **97**, 083507 (2005)
2. A. Mandelis, M. Pawlak, C. Wang, I. Delgado-Holfort, J. Pelzl, *J. Appl. Phys.* **98**, 123518 (2005)
3. J. Tolev, A. Mandelis, M. Pawlak, *J. Electrochem. Soc.* **154**(11), H983–H994 (2007)
4. A. Mandelis, *Solid State Electron.* **42**(1), 1–15 (1998)
5. M. Pawlak, M. Maliński, *Opto-Electron. Rev.* **22**(1), 31–35 (2014)
6. D. Dietzel, J. Gibkes, S. Chotikaprakhan, B.K. Bein, J. Pelzl, *Int. J. Thermophys.* **24**(3), 741–755 (2003)
7. X. Zhang, B. Li, X. Liu, *J. Appl. Phys.* **104**, 103705 (2008)
8. J. Schmidt, *IEEE Trans. Electron Devices* **46**(10), 2018–2025 (1999)
9. T. Creazzo, B. Redding, E. Marchena, S. Shi, D.W. Prater, *Opt. Lett.* **35**(21), 3691–3693 (2010)
10. Q. Huang, B. Li, *Rev. Sci. Instrum.* **82**, 043104 (2011)
11. Q. Huang, B. Li, *J. Appl. Phys.* **109**, 023708 (2011)
12. Ł. Chrobak, M. Maliński, *Elektronika - technologie, konstrukcje, zastosowania LIII* **12**, 110–113 (2012)
13. M. Pawlak, M. Maliński, *Infrared Phys. Technol.* **63**, 6–9 (2014)
14. M. Nestoros, Y. Karmiotis, C. Christofides, *J. Appl. Phys.* **82**(12), 6220–6227 (1997)